

A Comparison Between Square and Hexagonal Sampling Methods for Pipeline Image Processing.

Richard C. Staunton and Neil Storey

The University of Warwick, Coventry, UK, CV4 7AL.

ABSTRACT

The majority of machine vision systems derive their input data by digitising an image to produce a square grid of sampled points. However, other sampling techniques can represent equal picture information in a smaller number of samples, with a consequent reduction in data rate. Several workers have looked at regular hexagonal sampling of images which produces optimum data rates for a given information content. Previous work on hexagonal sampling by the authors and others, has shown that image processing operators are computationally more efficient, and as accurate, as their square counterparts.

Historically, one factor which has led to the predominance of square sampling in vision systems, is that this produces images which are more visually pleasing to human observers. This paper describes an investigation of machine vision systems performing industrial inspection tasks, which suggests that in such applications, hexagonal systems out-perform square systems. In particular hexagonal operators can follow tight curves more accurately, allowing better surface defect detection. A surprising observation of this work was that with such images, hexagonal sampling also gave images which were more visually pleasing to human operators.

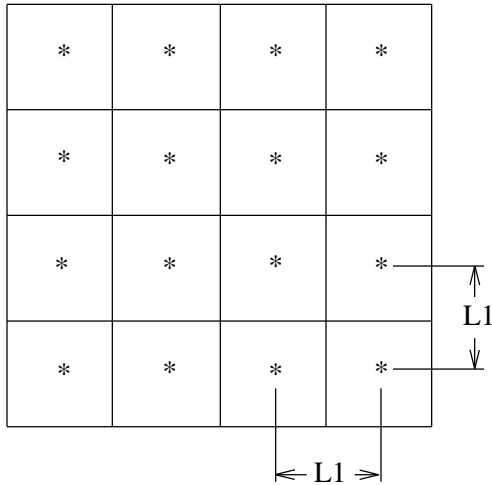
The paper presents a study of sampling point geometry and operator design. Details are given of an implementation of a set of hexagonal, grey-scale operators for use in pipeline or other image processing systems, and a comparison of square and hexagonal techniques has been made. Results of operations on real and simulated surface defect images are given for both sampling systems and the requirement for a defect detection figure of merit identified.

1. INTRODUCTION

Conventionally, images are digitised and stored as a square or rectangular array of values. The image is sampled at each point on a two dimensional grid of sampling points and a square or rectangular tiling of pixels applied to the grid such that a sampling point is located at the centre of each pixel. Before sampling, the image data is band limited in two dimensions in accordance with the sampling theorem. This is usually achieved through the averaging caused by the finite size of the sensing element. The area represented by the pixel is considered to have a uniform intensity of the value as measured at the sampling point at its centre. Such a grid of sampling points and pixels is shown in figure 1.

Many other sampling schemes are possible, some are listed by Whitehouse¹, but Mersereau² has shown that a regular hexagonal scheme is optimum for sampling circularly band limited two dimensional signals, in that the least number of sampling points are required to maintain equal high frequency information. 13.4% fewer points are required than for square sampling. On a regular hexagonal grid, sampling points are equidistant from each of their six nearest neighbours. The grid geometry is shown in figure 2.

Various pixel shapes can be considered to tile the hexagonal grid, hexagonal and rectangular being the most widely used. Rectangular pixels have the advantage for images displayed on raster scanned output devices, such as TV, monitors as the pixel height can be an integral number of scan lines. A rectangular pixel shape is shown in figure 2. If each pixel has unit height, then its length will be $2/(3^{1/2})$.



$$L1 = 1.0, \quad L2 = 2.0 / (3.0^{1/2}).$$

Figure 1. Square Pixels on a Square Grid.

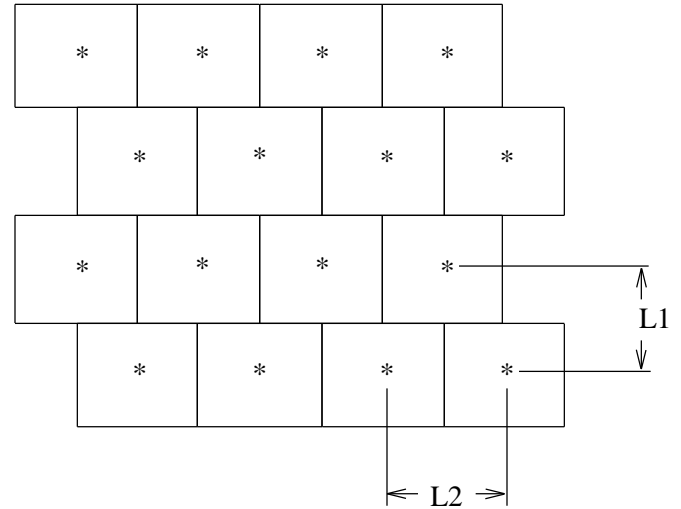


Figure 2. Rectangular Pixels on a Hexagonal Grid.

Local operators are easier to design for the hexagonal grid as the geometry constrains sampling points in the neighbourhood of a central point to be in fewer equidistant groups from the central point than in the square case. Distance from the centre is an important factor in local operator design. Figure 3 shows a local operator approximations to a Gaussian smoothing filter for use in the two systems. The area covered by the two operators is nearly the same, but the four corner points in the square operator are $2^{1/2}$ further from the centre than the other four neighbouring points. This has resulted in three weighting factors needing to be calculated, whereas for the hexagonal case, the six neighbours are equidistant from the centre and only two weighting factors needed to be calculated.

Connectivity within binary images has been shown by Golay³ to be more easily defined for hexagonally tiled images. The central pixel connects to each of its six neighbours along an equal length edge, whereas in the square system, connectivity can be edge to edge with the nearest four neighbours or additionally include corner to corner connectivity with the next nearest four. With a rectangular tiling on a hexagonal grid, connectivity can be visualised as end to end or half edge to half edge, but the computer connectivity model can revert to Golay's original definition.

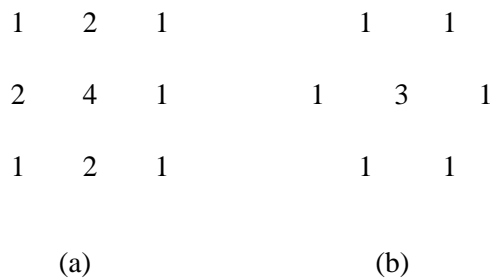


Figure 3. Gaussian Approximation Filters. (a) Square Grid. (b) Hexagonal Grid.

The class of image operators considered in this paper are all local operators, as these are easily realisable with a pipeline processor. These operators take as inputs the pixel values surrounding a particular pixel and output a new value for

that pixel. For completeness, we note that global operations are also possible on hexagonally sampled images. Mersereau² has developed a hexagonal f.f.t. and f.i.r. filters and shown these to be more computationally efficient than their square counterparts.

We have designed and simulated a pipeline architecture that will operate in real-time on a stream of video data input directly from a raster-scan device. All processes performed are local and so operators can be performed with only a few scan lines delay. The system and architecture are described in detail elsewhere^{4,5}, but essentially the pipeline processor system appears as in figure 4. The input is digitised and fed into the first processor element (PE) in a string of hardware identical PEs. Each PE is programmed to perform an operation from a set including edge detection, filtering, line thinning, inversion and scaling. Special features of the system include adaptive control and VLSI implementation of the PE. We envisage its use in high speed low cost applications. Output is either to a high level processor or a TV monitor. The basic PE architecture is shown in figure 5. Digitised video is input into a line length delay which feeds a second line delay. The leftmost three pixels of each line together with the first three pixels of the third scan line are accessible by the operator processor. This is a systolic processor which modifies the value of the central pixel of the nine pixels input to it. Thus the overall PE delay is one scan line plus a few extra pixels. This paper discusses how the architecture can accommodate hexagonally sampled images.

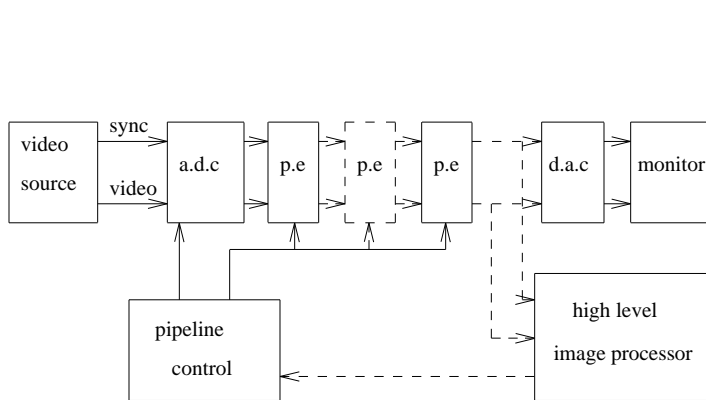


Figure 4. The Image Processor Pipeline.

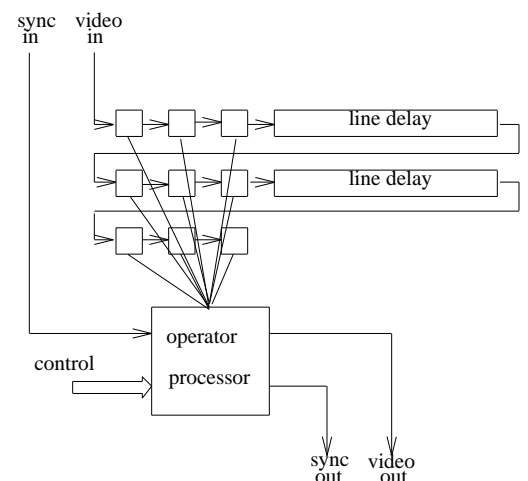


Figure 5. The Processor Element Architecture.

This paper considers the advantages and disadvantages of hexagonal sampling with respect to industrial inspection tasks and how such sampled images can be processed by a pipeline processor. Generally, the advantages include :-

- (a) That 13.4% fewer sampling points are required for equal high frequency information².
- (b) More efficient global² and local⁶ computation is possible.
- (c) The ease of defining connectivity³.
- (d) The ease of designing operators⁷.

The disadvantages include :-

- (a) The large number of published techniques specific to square sampled systems, although it is easy to design operators for the hexagonal system, time may be needed to convert published square system operators. Mersereau² notes that square two dimensional operators can easily be developed from one dimensional operators and that historically this led to the adoption of the square system.
- (b) Preston⁸ indicates that the main reason for the unpopularity of hexagonal systems would appear to be that it is perceptually more satisfactory for humans to observe straight vertical features on a square grid system, and that in

the real world, such features predominate. With a machine vision system, this will not be a concern as human involvement is limited to problem evaluation and system setup checking. We also note in this paper that under some circumstances hexagonal pixel images can be more pleasing to humans.

2. MODIFICATIONS TO THE PIPELINE FOR HEXAGONAL SAMPLING

2.1 System Modification

Considering the non-interlaced, analogue signal, TV camera as being the most likely input device to the pipeline, generally few system modifications are required to enable hexagonal digitisation of the signal. The signal must be circularly band limited at the same frequency as for an equal resolution square system, and as with square sampling, the vertical sampling point spacing is set to an integral number of scan lines. The horizontal sampling spacing is increased by a factor of $2/(3^{1/2})$, and the first sampling point on alternate lines delayed by half a point spacing. This reduces the number of points per scan line by the $2/(3^{1/2})$ factor. It is noted that the type of CCD camera that outputs a digital byte for each cell of its CCD array would require a modification to its array layout to enable hexagonal sampling.

The pipeline architecture is a systolic system and data input must be synchronised with the clock that pulses the line of processors that operate on the stream of data as it passes through. Fewer modifications to the PE result if the input data is arranged to synchronise with the PE as designed for square sampling. This is achieved if an A to D converter that converts in half the hexagonal sampling point spacing time is used. The converter samples at times so as to effect hexagonal sampling, but data is read at times to effect a rectangular array. This is illustrated in figure 6. Simple circuitry is used to re-synchronise the pipeline output data for display on a TV monitor.

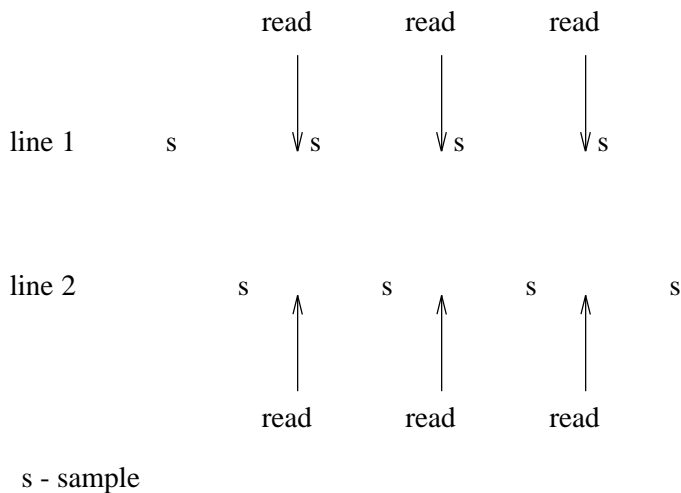


Figure 6. A to D Converter Sample and Data Ready Timing.

2.2 PE Modification

Changes to the PE architecture are minimal, extra taps are added to the line delays to reflect the reduced number of pixels per line. The operator processor must also be modified. For square sampled data, some operations performed by the processor require the convolution of the nine image pixels input to the processor with one or more 3×3 arrays of constants stored within the processor. The equivalent for hexagonally sampled data requires convolution with a seven element array, ie. a central element together with six surrounding elements. With the above system modifications, for hexagonal data, the position of the central pixel with respect to the six neighbours changes within the grid of nine input pixels on alternate scan

lines. This is illustrated in figure 7.

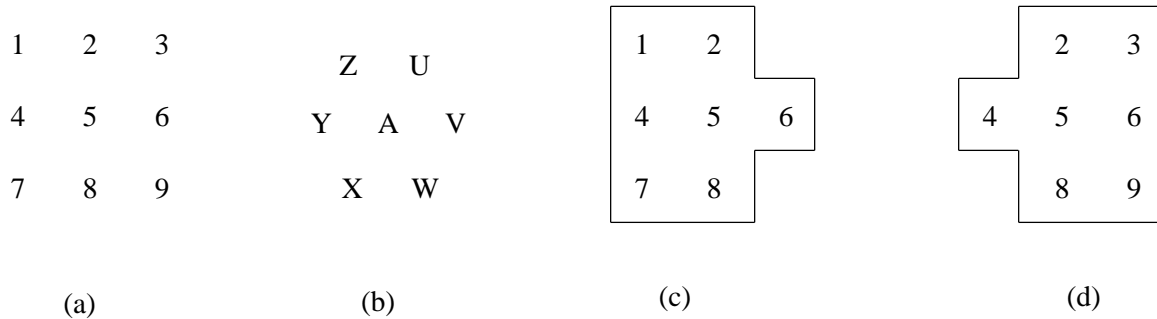


Figure 7. The Relationship Between the 9 Input Pixels and the 6 Hexagonal Nearest Neighbours on Alternate Scan Lines. (a) The 9 Input Pixels, (b) Logical Central Pixel A and 6 Nearest Neighbours, (c) Physical Set of 7 Pixels, Scan Line 1, (d) Physical Set of 7 Pixels, Scan Line 2.

It is necessary to store an extra set of convolution constant arrays within the PEs operator processor and to toggle between sets on alternate lines. The two unwanted elements in each array are set to zero. The extra area on a VLSI chip for these modifications is small in comparison to the area required by, for example, the line delays.

2.3 Comment

With a pipeline processor, the processing time for an image will be unaltered for a particular operation whether square or hexagonal digitisation is employed. One image is processed in one frame time, although a latency delay period is introduced by the string of PEs in the pipeline. The only advantages of hexagonal digitisation in pipelined systems is that the line delays can be reduced in length by 13.4% and that the PE master clock can be reduced by the same factor. These advantages will not greatly affect the final cost of the VLSI device, the argument has to be that a square only or a dual standard device looks likely for fabrication.

It will only be worth building an optional hexagonal processing capability into the PE if certain processes can be demonstrated to give better results with hexagonal data. The detection of small surface defects in industrial components is possibly such a process. It is noted that with a conventional single CPU computer, computation time savings of over 40% have been achieved with hexagonally sampled data⁶.

3. INSPECTION OF SURFACES FOR SMALL DEFECTS

To be used for industrial inspection tasks, machine vision systems must be cost effective, fast enough to process one object before the next one is presented and reliable. Pipeline systems employing VLSI - PEs are likely to be both cost effective and fast enough. Reliability of defect detection will now be considered. For a typical object accept-reject inspection application, it will be required to know the size of defect at which rejection should occur, then knowing the size of the complete object and the resolution of the system, the number of images required to cover the object can be calculated. If the number of images is minimised, the cost per object is minimised. The question of resolution must therefore be analysed.

In a noise free environment, even a sub-pixel size defect casting a shadow may have a detectable effect on the value of a pixel, but in a noisy environment false accept-reject decisions will occur. Slightly larger defects may produce effects in a group of neighbouring pixels, this group may still be unconnected, but their proximity can be used to decrease the number

of incorrect accept-reject decisions. Still larger defects may be detected as bounded regions and measurements of area and shape made to aid the accept-reject decisions and provide diagnostic information for the industrial process.

Theoretically we expect the hexagonal system to show advantages with small defect detection. Firstly, as the local operators used are more compact, they should follow tightly curved edges more easily, and secondly, the connectivity definition should enable easier outlining.

Figure 8. Square Sampled Image Showing Defects.

Figure 9. Hexagonal Sampled Image Showing Defects.

Figure 10. Edge Detected and Thinned Square Image.

Figure 11. Edge Detected and Thinned Hexagonal Image.

To test defect detectability we began by processing some images of defects in a sand core used for automobile engine castings. The defects consist of long scratches and roughly circular indentations of various sizes, the smallest being about 1mm. diameter. The entire object was 400mm. long. Figure 8 shows a zoom in on a part of the object resulting in a 64x64

square sampled image, the entire object was digitised as a 512x512 image. Figure 9 shows the equivalent hexagonally sampled section. These images were formed by averaging from an image of twice the resolution, this image consisted of rectangular pixels with a 4:3 aspect ratio, and it should be noted figure 8 is not a square sampled image, and that figure 9 is not a true 'regular' hexagonal sampled image. They can only give pointers to the possible advantages and disadvantages of the two systems. Figures 10 and 11 show the defect images after edge detection and thinning.

Three defects are visible in the grey scale images of the sand core, two circular defects are visible in the left finger of the core and a long scratch in the right finger. A strong light source was placed on the left side of the object, and a "fill in" source on the right side during imaging. Surface indentations are revealed by shadows on their left sides and bright areas on their right sides. This is not too easily seen in the PMT images published here, but is more easily discernible in the hexagonally sampled image. In the hexagonal image, the circular shape of the left finger defects are easier to discern as is the continuous scratch in the right finger, which is about three centimetres long. We also observe that, at this resolution, the near vertical object edges are more easily viewed in the hexagonal image.

When the images are edge detected and thinned, the resulting hexagonal image shows a well connected and parallel sided representation of the long scratch, whereas connectivity is incomplete and the shape not so easy to determined in the square image. For the large circular defect, connectivity is equivalent in the two images, but the indication of shape appears better in the hexagonal image. In both cases the third defect is indicated only by a collection of points.

The images were processed by a computer simulation of the pipeline⁴ which was modified to enable comparable square and hexagonal processing. An equivalent set of square and hexagonal local operators was assembled. Operators included:-

- (a) Edge detectors
- (b) Smoothing filters
- (c) Line thinners
- (d) Image inverter

The Sobel edge detector was extensively used as it has been demonstrated by Davies⁸ design principle to be nearly optimum for the square grid system, and an equivalent hexagonal operator has been designed by one of the authors^{6,7} to the same principles. A square system Gaussian approximation filter¹⁰ and its hexagonal equivalent⁷ were used for image smoothing and equivalent line thinning operators were developed.

The results from the sand core images appear to show some advantages for hexagonal processing, but the advantage must be shown on true square and regular hexagonally sampled images as the edge detectors and other operators have been optimally designed for these. We have continued to simulate such defects from mathematical models.

4. DEFECT MODELING AND DETECTION

4.1 The Model

The model is implemented on a computer. Its aim is to produce two output images, one on a square 16x16 grid, and the other on a 13x16 hexagonal grid that are representations of a precisely positioned and sized shape that has been input at the start of the computer programme. At present, two defect shapes are implemented, a circle and a rectangle. These can be of arbitrary size and position in the output images to within an accuracy of 0.03 of the length of a square pixel side. These shapes were chosen because they closely represent the defects found in the sand core image, a scratch being a long thin rectangle. Other shapes will be implemented as required.

Within the computer model the outline of the requested shape is plotted on a 512x512 square pixel grid and then each pixel is modified by other parameters such as background and defect brightness. When complete, this defect image is

averaged to produce the output images. A local area of 32x32 pixels is averaged to produce one square output pixel and an area of 37x32 pixels to produce one hexagonal output pixel. With images of this resolution, averaging of a integral number of pixels produces no distortion to the square and only very little to the hexagonal grid. This method produces a pair of, almost exactly, comparable images with which to test the square and hexagonal systems, although the total area covered by the hexagonal image is slightly less than that covered by the square image.

A simple model will contain the specified shape with the background brightness set at one value and the defect brightness set to another. Where a pixel straddles the background-defect border it will take an intermediate brightness value. A 3D plot of such a defect is shown in figure 12. A close examination of actual defects revealed the defects edges to be spread over several pixels in the transition from defect to background brightness. This effect is recreated in the model by smoothing the defect data before the actual output images are produced. Real images are noisy, and so noise of a predetermined variance can be added to the model data. A 3D plot of a defect, as in figure 12, but which has had its edges smoothed and noise added is shown in figure 13. A further sophistication can be added by dividing the defect into two segments, one which is brighter than the background and one darker. This models oblique illumination from one side of the object.

Figure 12. 3D Plot of Circular Defect.

Figure 13. 3D Plot of Circular Defect with Smoothed Edges and Added Noise.

4.2 Detection

Applying edge detectors to various modelled defects reveals results in close agreement with those obtained from the sand core images in section 3. However, many variables in the detection process have been identified and the overall question remains: Will a hexagonally sampled system enable quicker and more exact detection for a large class of defects? Defect detection is discussed in section 3, where three of many possible definitions are given. The choice of definition is task dependent and additionally many other variables are introduced by the processes that are used to achieve them. These variables have to be considered before a comparison can be made between defect detection on square and hexagonal grid images. For a detection scheme that involves defect outlining, variables include :-

- (a) The edge detector. The square and hexagonal detectors used in section 3 are equivalent for use in both systems, but they were designed to be optimal for straight step edges. With defects, tightly curved non-step edges, that may be considered planar only over small local areas, are likely to predominate, and this may lead to different detectors being designed. Step and planar edges are defined by Haralick¹¹.
- (b) The defect position and size. The position and size of small defects with respect to the digitisation grid makes a large difference to the edge detector output. A defect at a particular position may line up more optimally with, say, the square grid than the hexagonal grid of sampling points.
- (c) The defect shape. Some shapes will line up more optimally with a particular grid.

- (d) The connectivity definition. Two definitions are available for the square system.
- (e) The environmental and system noise. Noise will add uncertainty to the detection processes. In some cases, image filtering stages will need to be employed.
- (f) The percentage of complete outline necessary for detection. It may be possible to detect a defect and estimate its area and position without complete connectivity having been achieved.
- (g) The threshold method and value. The process may not be able to use optimum values.

To consider the effects of these variables, a 'Defect Detection Figure of Merit' algorithm (DDFOM) is currently being designed. A figure of merit method has been developed by van der Heyden¹² for edge detectors, which involves applying detectors to randomly generated images of straight edges and curves. We intend to derive our DDFOM from the detection of a series of randomly generated defect images and to link this with computation cost figures. We expect the information gained will enable us to identify defect detection as an application where hexagonal sampling can be advantageously employed and that a pipelined processing system is suitable. More widely, the DDFOM will provide general information for inspection system designers such as the detection probability of a certain size of defect.

5. CONCLUSIONS

For the industrial inspection application studied, the hexagonal grid processing system was able to outline defects at least as reliably, and for all the cases tried, more accurately, than the equivalently engineered square processing system. However, the more industrially useful tasks of defect typing and measurement will require additional, higher level processes, that, again, will have to be equivalently designed in order to compare the two systems. Many variables must be considered in order to make a useful comparison, and many processing operators, defect types, and computer architectures are available. Work has started to identify a defect figure of merit (DDFOM) algorithm and to link this to a computation cost figure. The DDFOM will not only indicate if the hexagonal system has an advantage for a wide class of defects, but also indicate to the designer which operators perform optimally for individual defect detection applications.

Regarding the human perception of hexagonally sampled images, we have found that defects viewed on a hexagonal grid of pixels are represented more exactly than on the square. The eye tends to follow the vertical lines formed by the pixel boundaries in the square image and to divide the defect up into vertical strip segments. In the hexagonal image, the eye seems to integrate information from all the defect pixels and convey a better representation of size and shape. These are only personal observations, and are not meant as a definitive comment on human perception. None of the images in this study contained perfectly vertical edges, but some long, near vertical edges were present (figures 8 and 9). At the resolution of these zoomed in images (64x64) these edges become smeared by the square pixel system, whereas in the hexagonal pixel system, it is easier for the eye to follow the edge. We conclude that hexagonally sampled industrial defect images are more pleasing to human observers. Preston⁸ noted that for general image viewing, the reverse is considered to be true, as many actual world images contain a preponderance of vertical edges.

The pipeline system can be easily modified to accommodate hexagonally sampled data. Only minor modifications, requiring little extra chip area, would be required to the VLSI processor element (PE) to enable a dual hexagonal-square image processing capability. A hexagonal only system would require approximately 13% less chip area and a lower clock rate than an equivalent square only system, but development cost will be minimised if only the one, dual purpose, system is pursued. The pipeline system simulation and all the hexagonal local operators designed worked well, and this together with the encouraging results from the surface defect application have convinced us to continue with the hexagonal processing option for our pipeline processor design.

6. REFERENCES

1. D.J.Whitehouse and M.J.Phillips, "Sampling in a two-dimensional plane," *J. Phys. A. Math. Gen.* vol. 18 pp. 2465-2477, 1985.

2. R.M.Mersereau, "The processing of hexagonally sampled two dimensional signals," *Proc. IEEE* vol. 67 no. 6 pp. 930-949, June 1979.
3. M.J.E.Golay, "Hexagonal parallel pattern transformations," *IEEE Trans. Computers* vol. C-18 pp. 733-740, Aug. 1969.
4. N.Storey and R.C.Staunton, "A pipeline processor employing hexagonal sampling for surface inspection," *3rd. Int. Conf. on Image Processing and its Applications*, IEE Conference Publication 307, pp.156-160, July 1989.
5. N.Storey and R.C.Staunton, "An adaptive pipeline processor for real-time image processing," *SPIE Conference: Automated inspection and high speed vision architectures 3, Philadelphia, USA. Proc. SPIE*, vol.1197, Nov. 1989.
6. R.C.Staunton, "The design of hexagonal sampling structures for image digitisation and their use with local operators," *Image and vision computing*, vol. 7, no. 3, pp. 162-166, Aug. 1989.
7. R.C.Staunton, "Hexagonal image sampling, a practical proposition," *Proc. SPIE* vol. 1008 pp. 23-27, 1989.
8. K.Preston et al. "Basics of cellular logic with some applications in medical image processing," *Proc. IEEE* vol.65, no.5, pp.826-856, 1979.
9. E.R.Davies, "Circularity a new principle underlying the design of accurate edge orientation operators," *Image and Vision Computing*, vol.2, no.3, pp. 134-142, Aug. 1985.
10. E.R.Davies, "Design of optimal Gaussian operators in small neighbourhoods," *Image and Vision Computing*, vol.15, no.3, pp 199-205, Aug. 1987.
11. R.M.Haralick, "Edge and region analysis for digital image data," *Computer Graphics and Image Processing* vol.12, no.1, pp.60-73, 1980.
12. F.van der Heyden, "Evaluation of Edge Detector Algorithms," *3rd. Int. Conf. on Image Processing and its Applications*, IEE Conference Publication 307, pp.618-622, July 1989.

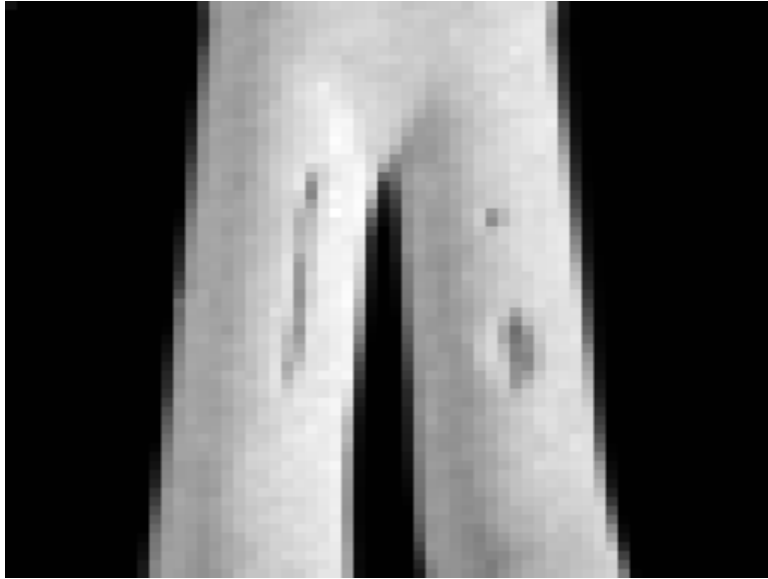


Figure 1: Fig 8. Square sampled image showing defects



Figure 2: Fig 9. Hexagonal sampled image showing defects.



Figure 3: Fig 10. Edge detected and thinned square image

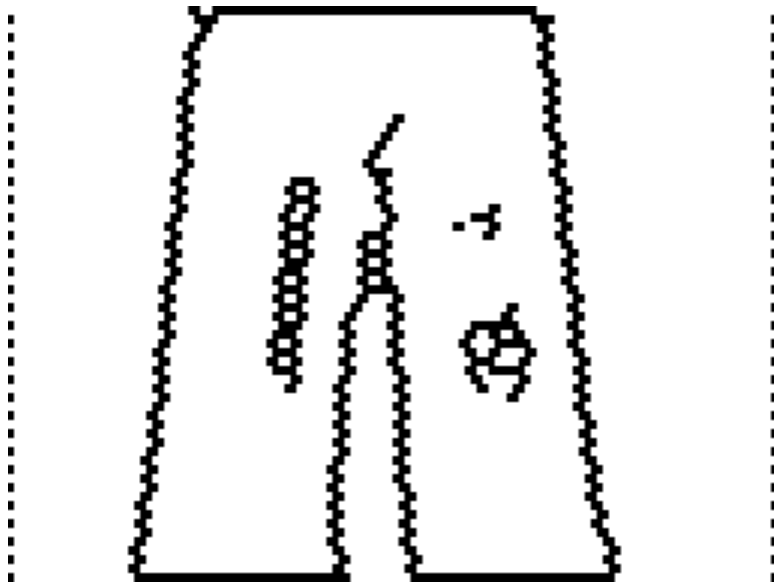


Figure 4: Fig 11. Edge detected and thinned hexagonal image

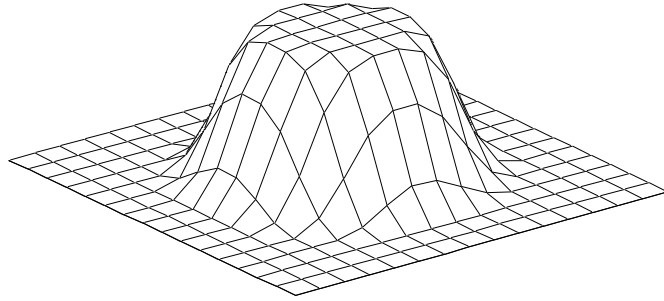


Figure 5: Fig 12. 3D plot of circular defect.

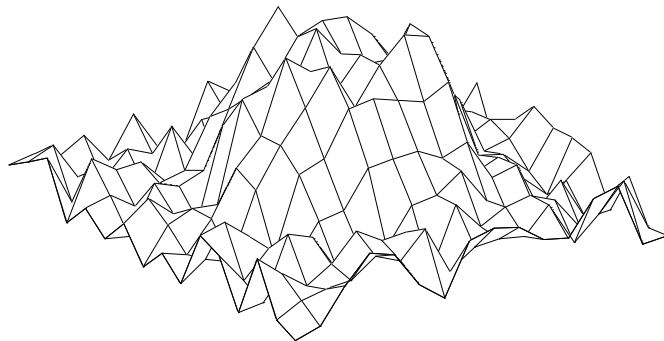


Figure 6: 3D plot of circular defect with smoothed edges and added noise